Chin. J. Astron. Astrophys. Vol. 7 (2007), No. 2, 304–316
(*http://www.chjaa.org*)

Chinese Journal of
Astronomy and
Astrophysics

Maser Emission of Relativistic Electrons Spiralling and Drifting in Curved Magnetic Fields *

Jiong Liu, Ye-Fei Yuan and Xiao-Long Deng

Center for Astrophysics, University of Science and Technology of China, Hefei 230026;
liujiong@mail.ustc.edu.cn

Received 2006 June 6; accepted 2006 September 3

Abstract Synchro-curvature radiation describes the emission from a relativistic charged particle which is moving and spiralling in a curved magnetic field. We investigate the maser emission for synchro-curvature radiation including drift of the guiding center of the radiating electron. It is shown that under some conditions the absorption coefficient can be negative, so maser can happen. These conditions are different from those needed for maser emission of curvature radiation including drift of the charged particles. We point out that our results, including the emissivity, can reduce to these of curvature radiation. Previously it was found that synchro-curvature radiation can not generate maser in vacuum, but we argue that synchro-curvature radiation including drift can generate maser even in vacuum. We discuss the possibilities of the potential applications of the synchro-curvature maser in modeling gamma ray bursts and pulsars.

Key words: masers — plasmas — radiation mechanisms: non-thermal

1 INTRODUCTION

Curvature and synchrotron radiations are essential for most models of pulsar radiation. In the curvature radiation mechanism, relativistic electrons and positrons in their lowest Landau orbits propagate along curved magnetic field lines, while in the synchrotron radiation mechanism the charged particles spiral around straight magnetic field lines. However, in the magnetosphere of the pulsar, charged particles not only move along curved magnetic lines, but also spiral around curved field lines, especially for those particles located near the light cylinder, which is about 10^3 times the stellar radius away from the center, and where the strength of the magnetic field is decreased significantly. Zhang & Cheng (1995) put forward a set of general radiation formulas for a relativistic charged particle moving in a curved magnetic field. This new radiation mechanism is named "synchro-curvature radiation mechanism" (Zhang & Cheng 1995; Cheng & Zhang 1996). In this new radiation mechanism the two key parameters are the curvature radius (ρ) and pitching angle (α). As $\rho \to \infty$ or $\alpha \to 0$, the synchro-curvature radiation reduces to synchrotron radiation or curvature radiation respectively, but it does not mean that curvature radiation requires $\alpha = 0$, instead, it requires $\sin^2\alpha \ll r_{\rm B}B/\rho$ (Cheng & Zhang 1996). In the original outer gap model for gamma ray pulsars, the curvature radiation from the accelerated electron-positrons moving along the last open field lines near the light cylinder accounts for the high energy radiation from the pulsars. However, even when the pitching angle is very small (e.g. $\sin\alpha \simeq 10^{-3}$), the radiation should, realistically, be synchro-curvature radiation (Zhang & Cheng 1997). For emitting particles located near the light cylinder, it is easy to derive the criteria for applying synchro-curvature radiation:

$$\sin\alpha = \frac{\gamma_6}{2BP}, \tag{1}$$

* Supported by the National Natural Science Foundation of China.

where γ_6 is the Lorentz factor in units of 10^6, B the strength of the magnetic field in Gauss, and P the rotational period of the pulsar in seconds. The synchro-curvature radiation has been generalized to the quantum limit (Zhang & Yuan 1998) and successfully applied to realistic astrophysical environments, such as gamma ray pulsars, gamma ray bursts, active galactic nucleus, and so on (Zhang & Cheng 1997; Zhang et al. 2000; Xia & Zhang 2001; Harko & Cheng 2002; Deng et al. 2005). The high radio luminosity of pulsars implies that their emission must be coherent. Maser will happen if an outgoing wave mode is amplified by an inversely populated electrons. Neglecting the curvature drift, Blandford (1975) proved that curvature maser emission is impossible. In 1979, Zhelezniakov argued that, if taking the effects of the curvature drift into account, maser emission is possible (Luo & Melrose 1992a, b). It has been proved that maser is impossible in vacuum if the effects of the drift of the guiding center are neglected (Yang et al. 2003). Zhelezniakov (1979) argued that a charged particle moving along a curved field line must be subject to some force which causes it to follow the curved path. Similarly, the guiding centers of the charged particles moving and spiralling in curved magnetic fields must drift. Cheng & Zhang (1996) also pointed out that the guiding center exists and the drift velocity exists only transverse to the magnetic field lines in the direction which is perpendicular to the plane that contains the field lines and the position vector. Including the drift of the guiding center, we show that the maser emission is possible even in vacuum. For simplicity, we do not consider the realistic shape of the magnetic field.

The most acceptable model for gamma-ray bursts (GRBs) is the fireball-shock model (for a recent review, for instance see Mészáros 2006), according to this model an energetic explosion drives a relativistic blast wave into an ambient gas (the forward shock), then the ejecta will interact with the surrounding medium and produce a relativistic shock back into the ejecta (the reverse shock). Most of the observations generally agree with the prediction of the model (Kulkarni et al. 2000), even though the model is incomplete. There are several problems which cannot be solved by observations, such as the burst progenitor and the physics of acceleration of electrons to high energies (Cheng & Lu 2001). The two dimensionless parameters, ξ_e and ξ_B, denoting respectively the fractions of shock internal energy density carried by relativistic electrons and by the magnetic field respectively, are not determined by the theory. Sagiv & Waxman (2002) have pointed that under their plausible assumptions on the electrons distribution function, synchrotron maser can happen and, together with other collective plasma effects in the radio emission from GRB afterglow, which can serve to constrain the value of ξ_B, as well as the parameters of the environment into which the fireball expands, thus providing a handle on both progenitor type and shock physics. Our recent research indicated that the new synchro-curvature radiation can be used to fit the spectra of GRBs better than synchrotron radiation (Deng et al. 2005), this means that the magnetic field is curved in GRB, the synchro-curvature maser should be considered instead of the synchrotron maser. If the maser happens, there should be a peak in the radio emission spectrum of the GRBs, and the frequency of the maser will be smaller than the generalized Razin-Tsytovich frequency v_R^* (Sagiv & Waxman 2002). In this paper we will give the detailed expression of the synchro-curvature maser that also includes the drift effect, because the guiding centers of the charged particles moving and spiralling in curved magnetic fields must drift, a realistic study should include the effects of the drift. More detailed discussion can be found in Section 6.

This paper is organized as follows. In Section 2 we describe the movement of the guiding center with drift and derive the expression for the total velocity of electrons. In Section 3.1 and 3.2 we derive the emissivity of radiating particles both in vacuum and in a plasma, and prove that our formulas reduce to those of synchro-curvature radiation if the effects of the drift are ignored, and that our formulas also reduce to those of curvature radiation including drift (Melrose 1978), if only the curvature drift is considered. In Section 4 we derive the absorption coefficient. The possibility of maser is discussed in Section 5. A discussion and potential applications are presented in Section 6.

2 EQUATION OF MOTION

We consider an electron with mass m and charge e moving and spiralling along a curved magnetic field line. Its guiding center moves along the magnetic field lines if without drift. First, we choose the Cartesian coordinates (x, y, z), the zero point is fixed on one magnetic field line, located in the (x, y)-plane. For convenience we also choose the cylindrical coordinates (ρ, φ, z). The relationship between these two coordinates is shown in Figure 1.

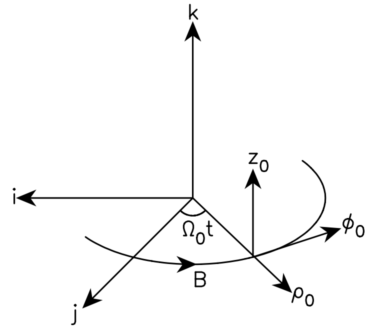

Fig. 1 Cartesian coordinates (x, y, z) and cylindrical coordinates (ρ, φ, z) used in this paper.

We assume when $t = 0$ the guiding center is on the y-axis. Let Ω_0 be its angular velocity, we have

$$\boldsymbol{\rho_0} = -\sin\Omega_0 t\boldsymbol{i} + \cos\Omega_0 t\boldsymbol{j}, \tag{2}$$

$$\boldsymbol{\varphi_0} = -\cos\Omega_0 t\boldsymbol{i} - \sin\Omega_0 t\boldsymbol{j}, \tag{3}$$

$$\boldsymbol{z}_0 = \boldsymbol{k}, \tag{4}$$

where $\boldsymbol{\rho_0}, \boldsymbol{\varphi_0}, \boldsymbol{z}_0$ are unit vectors of $\boldsymbol{\rho}, \boldsymbol{\varphi}, \boldsymbol{z}$; $\boldsymbol{i}, \boldsymbol{j}, \boldsymbol{k}$ are unit vectors of $\boldsymbol{x}, \boldsymbol{y}, \boldsymbol{z}$, respectively, and $\Omega_0 = v_\varphi/\rho = v\cos\alpha/\rho$. The equation of magnetic field line is

$$\boldsymbol{B} = B_0\boldsymbol{\varphi} = B_0\Big(\cos\varphi\boldsymbol{j} - \sin\varphi\,\boldsymbol{i}\Big). \tag{5}$$

The particle rotates in the (ρ_0, z_0)-plane, its position vector in the plane is

$$\boldsymbol{r} = r_B\cos\omega_B t\boldsymbol{\rho_0} + r_B\sin\omega_B t\boldsymbol{z_0}, \tag{6}$$

where $r_B = v\sin\alpha/\omega_B$ is its cyclotron radius, and $\omega_B = eB/(\gamma mc)$. In the Cartesian coordinates the position vector is

$$\boldsymbol{R} = \boldsymbol{r} + \boldsymbol{\rho},$$

where $\boldsymbol{\rho} = -\rho\sin\Omega_0 t\boldsymbol{i} + \rho\cos\Omega_0 t\boldsymbol{j}$. Using the relationship between these two coordinate systems, we have the total position vector,

$$\begin{aligned}\boldsymbol{R} = & -[\rho\sin(\Omega_0 t) + r_B\cos(\omega_B t)\sin(\Omega_0 t)]\boldsymbol{i} \\ & +[\rho\cos(\Omega_0 t) + r_B\cos(\omega_B t)\cos(\Omega_0 t)]\boldsymbol{j} \\ & +r_B\sin(\omega_B t)\boldsymbol{k}.\end{aligned} \tag{7}$$

Now we consider the drift of guiding centers. Because the guiding center can only have a drifting velocity transverse to the magnetic field line, the drifting velocity of the guiding center is along the z-direction, we can write the drift velocity as

$$\boldsymbol{v}_G = \frac{v^2\cos^2\alpha}{\omega_B\rho}\boldsymbol{z}_0 = \frac{\gamma m {v_\varphi}^2 c}{eB_0\rho}\boldsymbol{z}_0. \tag{8}$$

Thus the total velocity is given by $\boldsymbol{v} = \boldsymbol{v} + \boldsymbol{v}_G$. Including the drift, the total position vector is

$$\begin{aligned}\boldsymbol{R}_G = & -[\rho\sin(\Omega_0 t) + r_B\cos(\omega_B t)\sin(\Omega_0 t)]\boldsymbol{i} \\ & +[\rho\cos(\Omega_0 t) + r_B\cos(\omega_B t)\cos(\Omega_0 t)]\boldsymbol{j} \\ & +\left(r_B\sin(\omega_B t) + \frac{v^2\cos^2\alpha}{\omega_B\rho}t\right)\boldsymbol{k},\end{aligned} \tag{9}$$

and the total velocity including drift reads

$$\begin{aligned}\boldsymbol{V} = & - (\Omega_0\rho\cos(\Omega_0 t) - r_B\omega_B\sin(\omega_B t)\sin(\Omega_0 t) + r_B\Omega_0\cos(\omega_B t)\cos(\Omega_0 t))\boldsymbol{i} \\ & + (-\Omega_0\rho\sin(\Omega_0 t) - r_B\omega_B\sin(\omega_B t)\cos(\Omega_0 t) - r_B\Omega_0\sin(\Omega_0 t)\cos(\omega_B t))\boldsymbol{j} \\ & + \left(r_B\omega_B\cos\omega_B t + \frac{v^2\cos^2\alpha}{\omega_B\rho}\right)\boldsymbol{k}. \end{aligned} \tag{10}$$

As $t \to 0$, the approximate expression of the total velocity is given by

$$\begin{aligned}\boldsymbol{V} = & \quad (-\Omega_0\rho - r_B\Omega_0)\boldsymbol{i} + [(\Omega_0)^2\rho + r_B(\omega_B)^2 + r_B(\Omega_0)^2]t\boldsymbol{j} \\ & + \left(r_B\omega_B + \frac{v^2\cos^2\alpha}{\omega_B\rho}\right)\boldsymbol{k}. \end{aligned} \tag{11}$$

3 EMISSIVITY

A general formula for the energy radiated in the elemental range $\frac{d^3\boldsymbol{K}}{(2\pi)^3}$ at $\boldsymbol{K}$ due to an extraneous current is given by (Melrose 1978),

$$U^\sigma(\boldsymbol{K}) = 4\pi R_e{}^\sigma(\boldsymbol{K})\Big| e^\sigma(\boldsymbol{K})\cdot\boldsymbol{j}\Big[\boldsymbol{K},\varpi^\sigma(\boldsymbol{K})\Big]\Big|^2, \tag{12}$$

where $\boldsymbol{j}(K,\omega)$ is the Fourier transform of the current density. For the emission of transverse waves with refractive index $n = (1-\omega_p^2/\omega^2)^{1/2}$ (where ω_p is the plasma frequency, $\omega_p = 0$ if in vacuum). After summing over the two states of polarization, the above equation reduces to

$$U^t(\boldsymbol{K}) = 2\pi\Big(\Big|\frac{\boldsymbol{K}}{K}\times\boldsymbol{j}\Big[\boldsymbol{K},\sqrt{(\varpi_p^2+K^2c^2)}\Big]\Big|\Big)^2. \tag{13}$$

Suppose $j(\boldsymbol{K},\omega)$ is associated with a particle with charge e and mass m moving in an orbit $\boldsymbol{r} = \boldsymbol{r}(t)$, then $j(\boldsymbol{K},\omega)$ is defined as

$$\boldsymbol{j}(\boldsymbol{K},\omega) = e\int_{-\infty}^{\infty} dt\boldsymbol{v}(t)\exp\{i[\omega t - \boldsymbol{K}\cdot\boldsymbol{r}(t)]\}, \tag{14}$$

where the wave vector is defined as $\boldsymbol{K} = \frac{n\omega}{c}\boldsymbol{K}_0$, $\boldsymbol{K}_0$ is the unit vector of $\boldsymbol{K}$. The energy radiated per unit frequency and per unit solid angle is

$$U(\omega,\theta) = \frac{n\omega^2}{(2\pi c)^3}U^t(\boldsymbol{k}). \tag{15}$$

In order to simplify the calculation, we let $t \to 0$, then, without loss of generality, we assume the observer is located in the $(x,\, z)$-plane, and write θ_0 for the angle between the observer's position vector and $-\boldsymbol{i}$. So the unit wave vector is simplified to

$$\boldsymbol{K}_0 = -\cos\theta_0\boldsymbol{i} + \sin\theta_0\boldsymbol{k}. \tag{16}$$

In the following subsections, the general expressions Equations (12)–(15) are applied to obtain the emissivity of charged particles in vacuum and plasma conditions, respectively.

3.1 Emissivity for Single Particle in Vacuum

In vacuum, the refractive index n in $\boldsymbol{K}$ reduces to $n = 1$, then we have

$$\begin{aligned}\boldsymbol{K}\cdot\boldsymbol{r} &= \frac{\omega}{c}[\boldsymbol{K}_0\cdot\boldsymbol{r}] \\ &= \frac{\omega}{c}\Big\{\Big[(\rho+r_B)\Omega_0\cos\theta_0 + \left(r_B\omega_B + \frac{v^2\cos^2\alpha}{\omega_B\rho}\right)\sin\theta_0\Big]t \\ &\quad -\Big[(\rho+r_B){\Omega_0}^3\cos\theta_0 + 3\Omega_0{\omega_B}^2 r_B\cos\theta_0 + r_B{\omega_B}^3\sin\theta_0\Big]\frac{t^3}{6}\Big\}. \end{aligned} \tag{17}$$

In the above derivation, the following two approximations are used,

$$\sin\Omega_0 t \approx \Omega_0 t - \frac{1}{6}(\Omega_0 t)^3 \quad \text{and} \quad \cos\Omega_0 t \approx 1 - \frac{1}{2}(\Omega_0 t)^2. \tag{18}$$

Substituting Equation (17) into Equation (14) we have

$$\begin{aligned} \boldsymbol{j}(\boldsymbol{K},\omega) &= e\int_{-\infty}^{\infty} dt\boldsymbol{v}(t)\exp\{i[\omega t - \boldsymbol{K}\cdot\boldsymbol{r}(t)]\} \\ &= e\int_{-\infty}^{\infty} dt\boldsymbol{v}(t)\exp\{i[\omega t{Q_1}^2 + \frac{\omega v^3 t^3}{6c}{Q_2}^2]\}, \end{aligned} \tag{19}$$

where

$$\begin{aligned} {Q_1}^2 &= 1 - \frac{v}{c}\cos(\alpha-\theta_0) - \frac{v r_B}{c\rho}\cos\alpha\cos\theta_0 \\ &\quad - \frac{v^2\cos^2\alpha\sin\theta_0}{c\omega_B\rho}, \end{aligned} \tag{20}$$

$$\begin{aligned} {Q_2}^2 &= \frac{\cos^3\alpha\cos\theta_0}{\rho^2} + r_B\frac{\cos^3\alpha\cos\theta_0}{\rho^3} \\ &\quad + \frac{3\cos\alpha\sin^2\alpha\cos\theta_0}{\rho r_B} + \frac{\sin^3\alpha\sin\theta_0}{{r_B}^2}. \end{aligned} \tag{21}$$

We can prove that the right side of Equation (20) is greater than zero; in fact, the right side is related to the inclination angle χ between $\boldsymbol{v}$ and $\boldsymbol{K}$ when $t \approx 0$. In the cylindrical coordinates,$\boldsymbol{v}, \boldsymbol{K}$ can be written as

$$\begin{aligned} \boldsymbol{v} &= -r_B\omega_B\sin\omega_B t\boldsymbol{\rho_0} + (\rho + r_B\cos\omega_B t)\Omega_0\boldsymbol{\varphi_0} \\ &\quad + \Big(r_B\omega_B\cos\omega_B t + \frac{v^2\cos^2\alpha}{\omega_B\rho}\Big)\boldsymbol{z_0}, \end{aligned} \tag{22}$$

$$\boldsymbol{K} = \cos\theta_0\sin\Omega_0 t\boldsymbol{\rho_0} + \cos\theta_0\cos\Omega_0 t\boldsymbol{\varphi_0} + \sin\theta_0\boldsymbol{z_0}. \tag{23}$$

Thus,

$$\begin{aligned} \boldsymbol{K}\cdot\boldsymbol{v} &= -r_B\omega_B\cos\theta_0\sin\omega_B t\sin\Omega_0 t + (\rho + r_B\cos\omega_B t)\Omega_0\cos\theta_0\cos\Omega_0 t \\ &\quad + \Big(r_B\omega_B\cos\omega_B t + \frac{v^2\cos^2\alpha}{\omega_B\rho}\Big)\sin\theta_0 \\ &\approx v\Big\{\cos(\alpha-\theta_0) + \frac{r_B\cos\alpha\cos\theta_0}{\rho} + \frac{v\cos^2\alpha}{\omega_B\rho}\sin\theta_0\Big\} \\ &= v\cos\chi \approx v\Big(1 - \frac{1}{2}\chi^2\Big), \end{aligned} \tag{24}$$

and

$$\frac{1}{2}\chi^2 = 1 - \cos(\alpha-\theta_0) - \frac{r_B\cos\alpha\cos\theta_0}{\rho} - \frac{v\cos^2\alpha}{\omega_B\rho}\sin\theta_0. \tag{25}$$

The right side of Equation (20) can be expressed in terms of the inclination angle χ,

$$\begin{aligned} &1 - \frac{v}{c}\cos(\alpha-\theta_0) - \frac{v r_B}{c\rho}\cos\alpha\cos\theta_0 - \frac{v^2\cos^2\alpha\sin\theta_0}{c\omega_B\rho} \\ &\approx \frac{1}{2\gamma^2} + 1 - \cos(\alpha-\theta_0) - \frac{r_B}{\rho}\cos\alpha\cos\theta_0 - \frac{v^2\cos^2\alpha\sin\theta_0}{v\omega_B\rho} \\ &= \frac{1}{2\gamma^2} + \frac{1}{2}\chi^2 = {Q_1}^2 > 0. \end{aligned} \tag{26}$$

Applying the following integrals,

$$\int_{-\infty}^{\infty} dte^{i(\kappa t+at^3)} = \frac{2}{\sqrt{3}}\Big(\frac{\kappa}{3a}\Big)^{1/2}K_{1/3}\Big(\frac{2\kappa^{3/2}}{3(3a)^{1/2}}\Big), \tag{27}$$

$$\int_{-\infty}^{\infty} tdte^{i(\kappa t+at^3)} = \frac{2}{\sqrt{3}}\Big(\frac{\kappa}{3a}\Big)K_{2/3}\Big(\frac{2\kappa^{3/2}}{3(3a)^{1/2}}\Big), \tag{28}$$

the differential radiating power $U(\omega,\theta)$ can be expressed in terms of the modified Bessel functions,

$$\begin{aligned} U(\omega,\theta) &= \frac{\omega^2 e^2}{4\pi^2 c^3}\Big[\frac{4}{3}\Big((\rho+r_B)\frac{(v\cos\alpha)^2}{\rho^2}+r_B{\omega_B}^2\Big)^2 \\ &\Big(\frac{2{Q_1}^2}{c^2{Q_2}^2}\Big)^2\Big[K_{2/3}\Big(\frac{2\sqrt{2}\omega{Q_1}^3}{3cQ_2}\Big)\Big]^2+\frac{2}{3}\Big(\frac{2Q_1}{cQ_2}\Big)^2\Big[K_{1/3}\Big(\frac{2\sqrt{2}\omega{Q_1}^3}{3cQ_2}\Big)\Big]^2 \\ &\Big(v\cos\alpha\sin\theta_0+\frac{v^2\sin\alpha\sin\theta_0\cos\alpha}{\omega_B\rho}-v\sin\alpha\cos\theta_0-\frac{v^2\cos^2\alpha\cos\theta_0}{\omega_B\rho}\Big)^2\Big]. \end{aligned} \tag{29}$$

Finally, the expression for the emissivity is obtained,

$$\eta(\omega,\theta) = \frac{c}{2\pi\rho}U(\omega,\theta). \tag{30}$$

As expected, Equation (19) reduces to the corresponding result for the classical synchro-curvature radiation, when the effects of the drift of the guiding centers are neglected. Under this approximation,

$$\Big((\rho+r_B)\frac{(v\cos\alpha)^2}{\rho^2}+r_B{\omega_B}^2\Big)^2 \rightarrow \Big((\rho+r_B)(\Omega_0)^2+r_B{\omega_B}^2\Big)^2, \tag{31}$$

$$\begin{aligned} &\Big(v\cos\alpha\sin\theta_0+\frac{v^2\sin\alpha\sin\theta_0\cos\alpha}{\omega_B\rho}-v\sin\alpha\cos\theta_0-\frac{v^2\cos^2\alpha\cos\theta_0}{\omega_B\rho}\Big) \rightarrow \\ &(\rho+r_B)\Omega_0\sin\theta_0-\cos\theta_0 r_B\omega_B, \end{aligned} \tag{32}$$

$$(Q_1)^2 \rightarrow 1-\frac{v}{c}\cos(\alpha-\theta_0)-\frac{vr_B}{c\rho}\cos\alpha\cos\theta_0, \tag{33}$$

and Q_2^2 remains unchanged. Consequently, $U(\omega,\theta)$ reduces to the result for the synchro-curvature radiation (Cheng & Zhang 1996).

The expression of $U(\omega,\theta)$ is very complex and should be simplified. To do so, we first introduce

$$L = \frac{mc^2}{eB} \approx \frac{1640}{(B/\mathrm{G})}\mathrm{cm}. \tag{34}$$

Furthermore, assuming γ is bigger than 100, the expression for the emissivity is simplified to

$$\begin{aligned} \eta(\omega,\theta) &= \frac{\omega^2 e^2}{8\pi^3 c^2\rho}\Big[\frac{16}{3}\Big(\frac{\cos^2\alpha}{\rho}+\frac{\gamma L\cos^2\alpha\sin\alpha}{\rho^2}+\frac{\sin\alpha}{L\gamma}\Big)^2\Big(\frac{{Q_1}^2}{{Q_2}^2}\Big[K_{2/3}\Big(\frac{2\sqrt{2}\omega{Q_1}^3}{3cQ_2}\Big)\Big]^2\Big)^2 \\ &+\frac{8}{3}\Big(\frac{{Q_1}^2}{{Q_2}^2}\Big)\Big[K_{1/3}\Big(\frac{2\sqrt{2}\omega{Q_1}^3}{3cQ_2}\Big)\Big]^2\Big(\sin(\theta_0-\alpha)-\frac{\gamma L\cos\alpha\cos(\alpha-\theta_0)}{\rho}\Big)^2\Big], \end{aligned} \tag{35}$$

where

$$\begin{aligned} {Q_1}^2 &= \frac{1}{2\gamma^2}+2\sin^2\Big(\frac{\alpha-\theta_0}{2}\Big) \\ &-\frac{\gamma\sin\alpha\cos\alpha\cos\theta_0 L}{\rho}-\frac{\gamma\sin\theta_0\cos^2\alpha L}{\rho}, \end{aligned} \tag{36}$$

$$\begin{aligned} {Q_2}^2 &= \frac{\cos^3\alpha\cos\theta_0}{\rho^2}+\frac{\gamma\sin\alpha\cos^3\alpha\cos\theta_0 L}{\rho^3} \\ &+\frac{3\cos\alpha\sin\alpha\cos\theta_0 L}{\rho\gamma}+\frac{\sin\alpha\sin\theta_0}{L^2\gamma^2}. \end{aligned} \tag{37}$$

For the curvature radiation, the pitch angle $\alpha = 0$, and θ_0 is also very small, then

$$Q_2{}^2 \simeq \frac{1}{\rho^2} \quad \text{and} \quad Q_1{}^2 \simeq \frac{1}{2}[\gamma^{-2} + (\theta - \theta_d)^2] \equiv \frac{\xi^{-2}}{2}. \tag{38}$$

Substituting Equation (38) into Equation (35) and setting $\alpha = 0$, the emissivity $\eta(\omega, \theta)$ reduces to

$$\eta(\omega,\theta) = \frac{e^2\omega^2\rho}{6\pi^3 c^2}\Big\{(\theta_0-\theta_d)^2[\xi^{-1}K_{1/3}(\frac{\omega\rho}{3\xi^3 c})]^2 + [\xi^{-2}K_{2/3}(\frac{\omega\rho}{3\xi^3 c})]^2\Big\}, \tag{39}$$

where

$$\theta_d \equiv \frac{v_G}{v_\varphi} \approx \frac{\gamma L}{\rho}. \tag{40}$$

It is not surprising to find that Equation (39) is the result for the curvature radiation with drift obtained by Luo & Melrose (1992b).

3.2 Emissivity for Single Particle in Plasma

If the electron density of a plasma is high enough, the effects of the plasma must be considered (see, for example, Cawthorne 1985). Then we have,

$$\boldsymbol{K} = \frac{n\omega}{c}\boldsymbol{K}_0 = \left(1 - \frac{\omega_p{}^2}{\omega^2}\right)^{1/2}\boldsymbol{K}_0, \tag{41}$$

where ω_p is the plasma frequency,

$$\omega_p = 2\pi\left(\frac{n_e e^2}{\pi m}\right)^{1/2} \approx 1.8\times 10^4 \pi\sqrt{n_e}, \tag{42}$$

where n_e is the electron density of the plasma. The emissivity in plasma condition can be deduced similarly to that in the vacuum condition discussed in Section 3.1, and the results are summarized as follows:

$$\begin{aligned}\eta(\omega,\theta) \;=\; & \frac{(1-\omega_p{}^2/\omega^2)^{1/2}\omega^2 e^2}{18\pi^3 c^2\rho}\Big[\frac{1}{3}\Big(\frac{\cos^2\alpha}{\rho} + \frac{\gamma L\cos^2\alpha\sin\alpha}{\rho^2} + \frac{\sin\alpha}{L\gamma}\Big)^2 \\ & \Big(\frac{Q_1{}^2}{Q_2{}^2}K_{2/3}{}^2\Big(\frac{2Q_1{}^3}{3\sqrt{3}cQ_2}\Big)\Big)^2 + \Big(\frac{Q_1{}^2}{Q_2{}^2}\Big)K_{1/3}{}^2\Big(\frac{2Q_1{}^3}{3\sqrt{3}cQ_2}\Big) \\ & \Big(\sin(\theta_0-\alpha) - \frac{\gamma L\cos\alpha\cos(\alpha-\theta_0)}{\rho}\Big)^2\Big],\end{aligned} \tag{43}$$

where

$$\begin{aligned}Q_1{}^2 \;=\; & \omega\Big[1-(1-\frac{\omega_p{}^2}{\omega^2})^{1/2}\Big[\frac{\gamma\sin\alpha\cos\alpha\cos\theta_0 L}{\rho} \\ & +\frac{\gamma\sin\theta_0\cos^2\alpha L}{\rho}\Big] + \frac{1}{2\gamma^2}\Big(1-\frac{\omega_p{}^2}{\omega^2}\Big)^{1/2}\Big],\end{aligned} \tag{44}$$

$$\begin{aligned}Q_2{}^2 \;=\; & \frac{c^2\omega}{6}\Big(1-\frac{\omega_p{}^2}{\omega^2}\Big)^{1/2}\Big[\frac{\cos^3\alpha\cos\theta_0}{\rho^2} + \frac{\gamma\sin\alpha\cos^3\alpha\cos\theta_0 L}{\rho^3} \\ & +\frac{3\cos\alpha\sin\alpha\cos\theta_0 L}{\rho\gamma} + \frac{\sin\alpha\sin\theta_0}{L^2\gamma^2}\Big].\end{aligned} \tag{45}$$

4 ABSORPTION COEFFICIENT

The absorption coefficient $\mu(\omega,\theta)$ is given by

$$\mu(\omega,\theta)=-\frac{(2\pi c)^3}{2c\omega^2}\int_0^\infty d\epsilon\frac{df(\epsilon)}{d\epsilon}\eta(\omega,\theta), \tag{46}$$

where $f(\epsilon)$ is the energy distribution of electrons. Assuming $f(\epsilon)$ and $\eta(\omega,\theta)$ satisfy the mathematical requirements, Equation (46) can be integrated partially, thus,

$$\begin{aligned}\mu(\omega,\theta) &= -\frac{(2\pi c)^3}{2c\omega^2}\Big[f(\epsilon)\eta(\omega,\theta)|_0^\infty-\int_0^\infty d\epsilon f(\epsilon)\frac{\eta(\omega,\theta)}{d\epsilon}\Big]\\ &= \frac{(2\pi c)^3}{2c\omega^2}\int_0^\infty d\epsilon f(\epsilon)\frac{d\eta(\omega,\theta)}{d\epsilon}.\end{aligned} \tag{47}$$

For a monoenergetic distribution of radiating particles, the absorption coefficient reduces to

$$\mu(\omega,\theta)=\frac{N_e(2\pi c)^3}{2c\omega^2}\frac{d\eta(\omega,\theta)}{d\gamma}\Big|_{\gamma_0}, \tag{48}$$

where N_e is the number density of electrons which, for simplicity, we choose $N_e=1$, and γ_0 represents their energy. In the following two subsections, the absorption coefficients in vacuum and in a plasma are calculated respectively, and we will focus on $\frac{d\eta(\omega,\theta)}{d\gamma}$.

4.1 Absorption Coefficient in Vacuum: Single Particle Treatment

Based on the emissivity for single particle in Section 3.1, we have

$$\begin{aligned}\frac{d\eta}{d\gamma} &= \frac{\omega^2e^2}{\pi^3c^2\rho}\Big[\frac{4}{3}\Big[\frac{\cos^2\alpha}{\rho}+\frac{\gamma\cos^2\alpha\sin\alpha L}{\rho^2}+\frac{\sin\alpha}{\gamma L}\Big]\Big(\frac{\cos^2\alpha\sin\alpha L}{\rho^2}-\frac{\sin\alpha}{\gamma^2L}\Big)\Big(\frac{{Q_1}^2}{{Q_2}^2}K_{2/3}\Big)^2+\\ &\frac{4}{3}\Big[\frac{\cos^2\alpha}{\rho}+\frac{\gamma\cos^2\alpha\sin\alpha L}{\rho^2}+\frac{\sin\alpha}{\gamma L}\Big]^2\Big(\frac{{Q_1}^2}{{Q_2}^2}K_{2/3}\Big)\Big(\frac{{Q_1}^2}{{Q_2}^2}K_{2/3}\Big)'+\\ &\frac{2}{3}\Big(\sin(\theta_0-\alpha)-\frac{\gamma\cos\alpha\cos(\alpha-\theta_0)L}{\rho}\Big)\Big(-\frac{\cos\alpha\cos(\alpha-\theta_0)L}{\rho}\Big)\Big(\frac{Q_1}{Q_2}K_{1/3}\Big)^2\\ &+\frac{2}{3}\Big(\sin(\theta_0-\alpha)-\frac{\gamma\cos\alpha\cos(\alpha-\theta_0)L}{\rho}\Big)^2\Big(\frac{Q_1}{Q_2}K_{1/3}\Big)\Big(\frac{Q_1}{Q_2}K_{1/3}\Big)'\Big].\end{aligned} \tag{49}$$

Applying the properties of the modified K-Bessel function,

$$\frac{d}{dz}(z^\nu K_\nu) = -z^\nu K_{\nu-1}, \tag{50}$$

$$\frac{d}{dz}(z^{-\nu} K_\nu) = -z^{-\nu} K_{\nu+1}, \tag{51}$$

$$K_v(z) = \frac{I_{-\nu}(z)-I_\nu(z)}{2\sin\nu}, \tag{52}$$

we obtain

$$\Big(\frac{Q_1}{Q_2}K_{1/3}\Big)' = -\frac{2Q_1K_{1/3}Q_2'}{3{Q_2}^2}-\frac{2\sqrt{2}\omega(3Q_2{Q_1}^3Q_1'-{Q_1}^4Q_2')}{3c{Q_2}^3}K_{2/3}, \tag{53}$$

$$\Big(\frac{{Q_1}^2}{{Q_2}^2}K_{2/3}\Big)' = -\frac{4{Q_1}^2K_{2/3}Q_2'}{3{Q_2}^3}-\frac{2\sqrt{2}\omega(3Q_2{Q_1}^4Q_1'-{Q_1}^5Q_2')}{3c{Q_2}^4}K_{1/3}, \tag{54}$$

where

$$Q_1{}' = -\frac{\sin\alpha\cos\alpha\cos\theta_0 L + \sin\theta_0\cos^2\alpha L}{2\rho Q_1} - \frac{1}{2\gamma^3 Q_1}, \quad (55)$$

$$Q_2{}' = \frac{1}{2Q_2}\Big(\frac{\sin\alpha\cos^3\cos\theta_0 L}{\rho^3} - \frac{3\cos\alpha\sin\alpha\cos\theta_0}{\rho\gamma^2 L} - \frac{2\sin\alpha\sin\theta_0}{L^2\gamma^3}\Big). \quad (56)$$

4.2 Absorption Coefficient in Plasma: Single Particle Treatment

Similar to the calculation in Section 4.1, based on the expression for emissivity in Section 3.1, we have

$$\begin{aligned}\frac{d\eta}{d\gamma} = & \frac{(1-\omega_p{}^2/\omega^2)^{1/2}\omega^2 e^2}{18\pi^3 c^2\rho}\Big[\frac{2}{3}\Big[\frac{\cos^2\alpha}{\rho} + \frac{\gamma\cos^2\alpha\sin\alpha L}{\rho^2} + \frac{\sin\alpha}{\gamma L}\Big] \\ & \Big(\frac{\cos^2\alpha\sin\alpha L}{\rho^2} - \frac{\sin\alpha}{\gamma^2 L}\Big)\Big(\frac{Q_1{}^2}{Q_2{}^2}K_{2/3}\Big)^2 + \\ & \frac{2}{3}\Big[\frac{\cos^2\alpha}{\rho} + \frac{\gamma\cos^2\alpha\sin\alpha L}{\rho^2} + \frac{\sin\alpha}{\gamma L}\Big]^2\Big(\frac{Q_1{}^2}{Q_2{}^2}K_{2/3}\Big)\Big(\frac{Q_1{}^2}{Q_2{}^2}K_{2/3}\Big)' + \\ & 2\Big(\sin(\theta_0-\alpha) - \frac{\gamma\cos\alpha\cos(\alpha-\theta_0)L}{\rho}\Big)\Big(-\frac{\cos\alpha\cos(\alpha-\theta_0)L}{\rho}\Big)\Big(\frac{Q_1}{Q_2}K_{1/3}\Big)^2 + \\ & 2\Big(\sin(\theta_0-\alpha) - \frac{\gamma\cos\alpha\cos(\alpha-\theta_0)L}{\rho}\Big)^2\Big(\frac{Q_1}{Q_2}K_{1/3}\Big)\Big(\frac{Q_1}{Q_2}K_{1/3}\Big)'\Big]. \end{aligned} \quad (57)$$

Use the properties of the modified K-Bessel function Equations (50)–(52), we get

$$\Big(\frac{Q_1}{Q_2}K_{1/3}\Big)' = -\frac{2Q_1K_{1/3}Q_2{}'}{3Q_2{}^2} - \frac{(6Q_2Q_1{}^3Q_1{}' - 2Q_1{}^4Q_2{}')}{3\sqrt{3}cQ_2{}^3}K_{2/3}, \quad (58)$$

$$\Big(\frac{Q_1{}^2}{Q_2{}^2}K_{2/3}\Big)' = -\frac{4Q_1{}^2K_{2/3}Q_2{}'}{3Q_2{}^3} - \frac{(6Q_2Q_1{}^4Q_1{}' - 2Q_1{}^5Q_2{}')}{3\sqrt{3}cQ_2{}^4}K_{1/3}, \quad (59)$$

where

$$\begin{aligned} Q_1{}' &= -\omega(1-\frac{\omega_p{}^2}{\omega^2})^{1/2}\Big[\frac{\sin\alpha\cos\alpha\cos\theta_0 L}{\rho} + \frac{\cos^2\alpha\sin\theta_0 L}{\rho}\Big]\frac{1}{2Q_1}, \\ Q_2{}' &= \frac{c^2\omega}{6}\Big(1-\frac{\omega_p{}^2}{\omega^2}\Big)^{1/2}\frac{1}{2Q_2}\Big[\Big(\frac{\sin\alpha\cos^3\cos\theta_0 L}{\rho^3} \\ &\quad -\frac{3\cos\alpha\sin\alpha\cos\theta_0}{\rho\gamma^2 L} - \frac{2\sin\alpha\sin\theta_0}{L^2\gamma^3}\Big)\Big]. \end{aligned} \quad (60)$$

So far, we have had the full expression of the absorption coefficient and its differential quotient. Then we are going to investigate whether or not maser takes place for electrons moving and spiralling in curved magnetic fields.

5 MASER

It is well-known that amplification of the acceleration emission of electrons occurs when the absorption coefficient is negative. Two conditions must be satisfied: one is

$$\frac{df(\epsilon)}{d\epsilon} > 0, \quad (61)$$

which means an inverted energy population. The other is

$$\frac{d\eta(\omega,\theta)}{d\epsilon} < 0. \quad (62)$$

This condition is needed according to Equation (47). If $\frac{d\eta}{d\gamma} < 0$ under some conditions, then the amplification can happen. It is found there are three conditions on the parameters needed for amplification, The first one is

$$\alpha \approx \theta_0 \ll 1, \qquad \text{but} \qquad \alpha \neq \theta_0. \tag{63}$$

This condition comes from the beaming effect of relativistic electrons. The second is

$$\frac{(\alpha-\theta_0)^2}{2} - \frac{\gamma L(\alpha+\theta_0)}{\rho} > 0. \tag{64}$$

If this condition does not hold, the phase factor of $\boldsymbol{j}(\boldsymbol{K},\omega)$ will oscillate rapidly, making the positive and negative shifts cancel each other. The third is

$$\sin\alpha \approx \frac{r_B}{\rho}. \tag{65}$$

This condition is needed by the synchro-curvature radiation.

The expressions which are associated with the absorption coefficient are so complex that numerical calculations are needed to check whether the "minus absorption" takes place or not. Figures 2–5 show the absorption coefficient (in arbitrary units) as a function of the radiating frequency, the Lorentz factor, the strength of the magnetic fields, and the curvature radius, respectively. The effects of the plasma are shown in Figure 6. In these figures, ω_c is the characteristic frequency of the synchro-curvature radiation:

$$\omega_c \;=\; \frac{3}{2}\gamma^3 c\Big(\frac{\cos^4\alpha}{\rho^2} + r_B\frac{\cos^4\alpha}{\rho^3} + \frac{3\sin^2\alpha\cos^2\alpha}{\rho r_B} + \frac{\sin^4\alpha}{{r_B}^2}\Big)^{1/2}. \tag{66}$$

According to Figures 2–6 and more numerical calculations not shown here, it is evident that, in vacuum, maser of synchro-curvature radiation including drift can happen in a little more relaxed condition than that of curvature radiation including drift. Our main conclusions are summarized as:

1. Comparing with the case of curvature radiation, effective amplification can occur in a higher frequency range. Our frequency range is from radio band to X-ray band, but in curvature radiation including drift, Luo & Melrose (1992a) concluded that the amplification needs $B > 1.6\times10^{-6}(\omega/\omega_R)^{1/6}(\omega^2/\omega_R)$ G. For example, for emission in the range 2–200 MHz, the magnetic field needs to be larger than 10^{8} G. If the frequency of the coherent emission is higher than 10^{14} Hz, the magnetic field may be inconceivably too strong, while for synchro-curvature radiation, amplification can happen in a weaker magnetic field. Figure 2 shows that the amplification happens at 1.0×10^{14} Hz with $B = 10^4$ G.
2. More numerical calculations show that the Lorentz factor needed by maser is smaller in our case than in the case of curvature radiation (see Fig. 3): $\gamma > 10^2$, whereas for curvature radiation including drift, Luo & Melrose (1992a) concluded that $\gamma \geq 10^3$.
3. For curvature radiation including drift, Luo & Melrose (1992a) concluded that curvature maser mechanism requires a strong magnetic field in the source region, especially at the stellar surface, whereas maser due to synchro-curvature radiation including drift can happen in a wider range of magnetic field and radius. Figures 4 and 5 show that the amplification can happen in magnetic fields $B < 10^3$ G when $\rho = 10^8$ cm, or in a magnetic field of $B = 10^4$ G when $\rho = 3\times10^8$ cm.
4. Figure 6 clearly shows the effect of plasma on the absorption coefficient. The effect is important only when the electron density is high, and only happens at frequencies below that of the maser.

6 DISCUSSION AND APPLICATION

Synchro-curvature radiation generally describes the emission from a relativistic charged particle which is moving and spiralling in a curved magnetic field (Zhang & Cheng 1995; Cheng & Zhang 1996). It has already been successfully applied to realistic astrophysical environments (Zhang & Yuan 1998; Zhang et al. 2000; Xia & Zhang 2001; Harko & Cheng 2002; Deng et al. 2005). GRB is a kind of short-time burst of gamma rays in the universe. Though the light curves of GRBs are extremely variable, their spectrum are fairly homogeneous, which makes them convenient for studying the radiation mechanism.

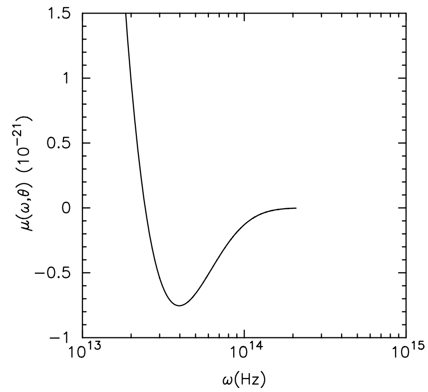

Fig. 2 Absorption coefficient $\mu(\omega, \theta)$ (in arbitrary units) as a function of frequency ω in the single particle treatment. A monoenergetic distribution of radiating particles is assumed, the Lorentz factor is taken to be $\gamma = 10^3$, the other parameters are taken to be $B = 10^4$ G, α=0.1 and ρ=10^8 cm.

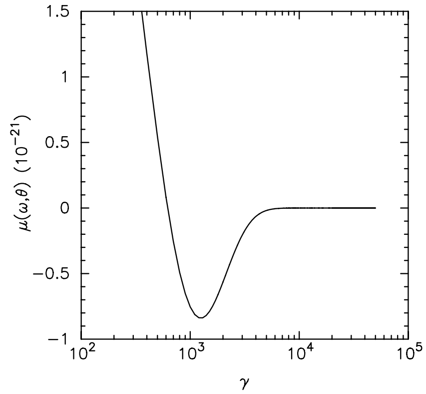

Fig. 3 Absorption coefficient $\mu(\omega, \theta)$ versus the Lorentz factor γ in the single particle treatment. The parameters are $B = 10^4$ G , $\alpha = 0.1$, $\rho = 10^8$ cm, $\omega = 4.0 \times 10^{13}$ Hz and $\omega_c = 3.6 \times 10^{16}$ Hz.

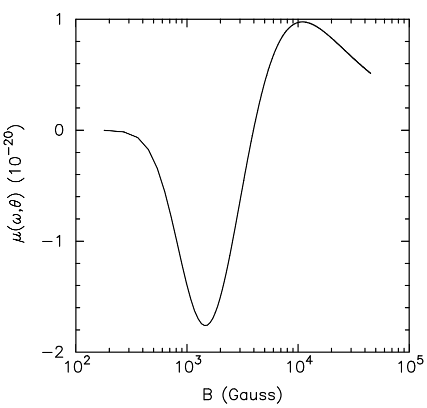

Fig. 4 Absorption coefficient $\mu(\omega, \theta)$ as a function of the strength of magnetic field in the single particle treatment. The parameters are $\gamma = 10^3$, $\alpha = 0.1$, $\rho = 10^8$cm, $\omega = 4.0 \times 10^{13}$Hz and $\omega_c = 3.6 \times 10^{16}$Hz.

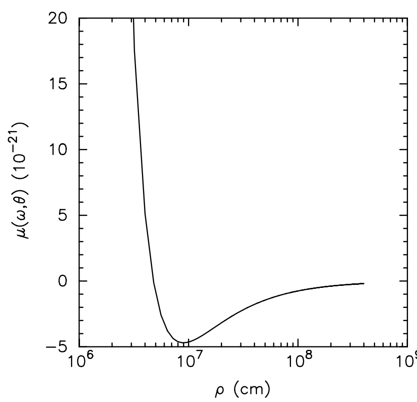

Fig. 5 Absorption coefficient $\mu(\omega, \theta)$ versus curvature radii in the single particle treatment. The parameters are $B = 10^4$ G, $\alpha = 0.1$, $\gamma = 10^3$, $\omega = 4.0 \times 10^{13}$ Hz and $\omega_c = 3.6 \times 10^{16}$ Hz.

The spectra are fitted phenomenologically by Band et al. (1993), and then Katz (1994) suggested that synchrotron emission is likely to be the radiation mechanism. The spectra of some GRBs were well fitted by synchrotron radiation from relativistic particles with a power law distribution (Tavani 1996), but in both the low and high energy bands the GRB spectrum often differs from that of the pure synchrotron radiation, urging people to study the GRB spectrum more carefully. Deng, Xia & Liu (2005) used synchro-curvature mechanism to study the prompt spectrum of GRBs and discussed some characteristics of synchro-curvature radiation in the internal shocks. The new radiation mechanism can fit the spectra of some GRBs very well, e.g., GRB930131, GRB910503, GRB910601, GRB910814 and GRB920622, etc. (Deng, Xia & Liu 2005). This indicates that the synchro-curvature radiation mechanism can be used to analyze the spectrum of GRBs, and that the magnetic fields of GRBs are curved, therefore, the curvature effect should be taken into account when investigating the maser emission in GRBs. The synchro-curvature radiation including drift discussed in this paper can be used to analyze the maser emission of GRBs either in vacuum or in a plasma.

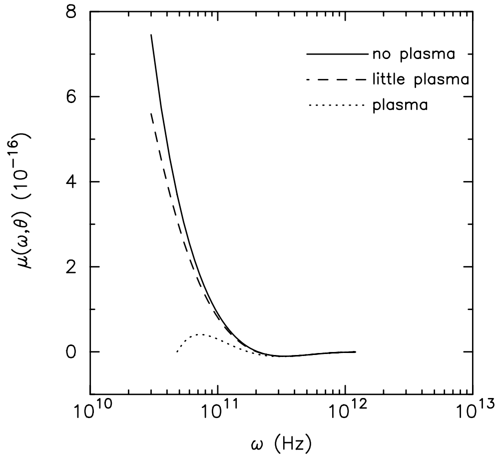

Fig. 6 Absorption coefficient $\mu(\omega, \theta)$ as a function of frequency ω. The parameters are $B = 10^3$ G, $\alpha = 0.1$, $\gamma = 200$, $\rho = 10^7$cm and $\omega_c = 3.6 \times 10^{14}$ Hz and $n_e \approx 10^9\,\mathrm{cm}^{-3}$ for dilute plasma condition, and $n_e \approx 10^{10}\,\mathrm{cm}^{-3}$ for plasma condition. In the plasma condition the plasma frequency ω_p is near the frequency range where the maser happens.

Both the frequency at which the synchrotron maser happens and the synchrotron characteristic frequency are related to ξ_e and ξ_B(Sagiv & Waxman 2002), though the relationship may vary a little in different scenarios of GRB fireball expansion. If maser emission is displayed in the radio emission spectrum of a GRB, it implies that the magnetic field of the GRB is weak, because the strong effect of the plasma can only happen under the condition $\frac{\nu_p}{\nu_B} \gg 1$. Using the relationships of $\nu_p \propto (\frac{\xi_e}{0.5})^{-1/2}$, $\nu_B \propto (\frac{\xi_e}{0.5})^{-1}(\frac{\xi_B}{10^{-6}})^{1/2}$, $v_c \propto (\frac{\xi_e}{0.5})^2(\frac{\xi_B}{10^{-6}})^{1/2}$ and $v_R^* \propto (\frac{\xi_e}{0.5})^{-1/4}(\frac{\xi_B}{10^{-6}})^{-1/4}$ shown by Sagiv & Waxman (2002), ξ_B will be constrained by $\xi_B \sim 10^{-6}$ which is much smaller than the common concept of ξ_B. These effects may serve as an important clue to the GRB environment and progenitor type. As the magnetic field of GRBs is curved, if we consider the synchro-curvature maser, ν_c and ν_R^* of the synchro-curvature radiation are different from those of synchrotron radiation. Using the relationship listed above, the values of ξ_e and ξ_B will be changed, then the constraint of ξ_B, as well as the other parameters of the environment into which the fireball expands, will be different from the constraint if the synchrotron maser is considered, but the detailed discussion of which is beyond the scope of this paper.

Pulsar is a magnetized, rotating neutron star. The geometric structure of the pulsar's magnetic field is approximately a dipole field. So the synchrotron radiation can only be used approximately because the magnetic field is curved. Moreover, not all electrons move along the magnetic field line, so the curvature radiation can only be used partly. A more precise radiation mechanism is synchro-curvature radiation because it can solve the radiation problem of electrons moving in a curved magnetic field relativistically or non-relativistically. The synchro-curvature radiation mechanism has already been applied to the thick outer gap model of pulsar (see Zhang & Cheng 1997) and yielded some good result. However, if without drift, a curved magnetic field will create a magnetic gradient, which generates a drift motion of the particles and gives a non-negligible contribution to the radiation spectrum (Harko & Cheng 2002).

Synchro-curvature radiation including drift, which is discussed in this paper, can be used to analyze pulsar's maser phenomenon both in vacuum and in a plasma. This kind of maser phenomenon is generated by the electron itself which is moving in the magnetic field.

In this paper, we have discussed maser emission of the synchro-curvature radiation including drift. Melrose (1978) has already pointed out that maser emission needs an inverted energy population. This sets a strong constraint on the energy distribution of electrons. It is safe to say that the famous power-law energy distribution can not generate maser. For simplicity, we choose a monoenergetic distribution of the radiating particles as an example to check the maser actions. A more realistic choice is the gauss distribution, which energy distribution includes an inverted energy population naturally. When the dispersion of the Gaussian distribution approaches zero, it reduces to the monoenergetic distribution.

Finally, we should point out that the magnetic field considered in this work is the one the strength of which is constant, but its field lines are curved. Such a field must be inhomogeneous, and the density of the magnetic field lines varies from point to point. So the inhomogeneity of the magnetic field creates a magnetic gradient, which generates a kind of transverse drift motion. The velocity of a charged particle moving in a curved inhomogeneous magnetic field is given by Jackson (1975),

$$\boldsymbol{v} = \boldsymbol{v}_0 + \frac{\gamma mc}{e}\frac{(v_0\cos\alpha)^2 + \frac{1}{2}(v_0\sin\alpha)^2}{\rho^2 B^2}\boldsymbol{\rho}\times\boldsymbol{B}, \tag{67}$$

and we have argued that $\alpha \ll 1$ is needed, so

$$\boldsymbol{v} \approx \boldsymbol{v}_0 + \frac{\gamma mc}{e}\frac{(v_0\cos\alpha)^2}{\rho^2 B^2}\boldsymbol{\rho}\times\boldsymbol{B} = \boldsymbol{v}_0 + \boldsymbol{v}_G \tag{68}$$

is a good approximation. It is due to this reason that we have neglected the gradient velocity in this paper .

Acknowledgements The authors would like to thank the anonymous referee for her/his constructive comments. This work is partially supported by the National Natural Science Foundation of China (Grants 10673010, 10233030 and 10573016), and the program for New Century Excellent Talents in University.

References

Blandford R. D., 1975, MNRAS, 170, 551
Band D.,Matteson L.,Ford L. et al., 1993, ApJ, 413, 281
Cawthorne T. V., 1985, MNRAS, 216, 795
Cheng K. S., Zhang J. L., 1996, ApJ, 463, 271
Cheng K.S., Lu T., 2001, Chin. J. Astron. Astrophys. (ChJAA), 1, 1
Deng X. L., Xia T. S., Liu J., 2005, A&A, 443, 747
Gao W. H, Wei D. M., 2005, Chin. J. Astron. Astrophys. (ChJAA), 5, 571
Harko T., Cheng K. S., 2002, MNRAS, 335, 99
Hirotani K., Harding A. K., Shibata S., 2003, ApJ, 591, 334
Jackson J. D., 1975, Classical Electrodynamics, 2nd ed., New York: Wiley, 1975
Katz J. I, 1994, ApJ, 422, 248
Kulkarni S. R. et al. 2000, the 5th Huntsville Gamma-Ray Burst Symposium
Luo Q., Melrose D. B., 1992a, MNRAS, 258, 616
Luo Q., Melrose D. B., 1992b, Proceedings of the Astronomical Society of Australia, 10, 45
Melrose D. B., 1978, ApJ, 225, 557
Mészáros P., 2006, Rep. Prog. Phys., 69, 2259
Sagiv A., Waxman E., 2002, ApJ, 574, 861
Sobolev Y. M, 2001, Kosmicheskaia Nauka i Tekhnika, 789
Tavani M., 1996, ApJ, 466, 768
Xia T.-S., Zhang J.-L., 2001, A&A, 371, 93
Yang J. M., Liu J., Zhang J. L., 2003, Journal of USTC, 33, 158
Zhang J. L., Cheng K. S., 1995, Phys. Lett. A, 208, 47
Zhang J.-L., Xia T.-S., Yang J.-M., 2000, Phys. Lett. A, 275, 315
Zhang J. L., Yuan Y. F., 1998, ApJ, 493, 826
Zhang L., Cheng K. S., 1997, ApJ, 487, 370
Zhelezniakov V. V., Shaposhnikov V. E., 1979, Australian Journal of Physics, 32, 49